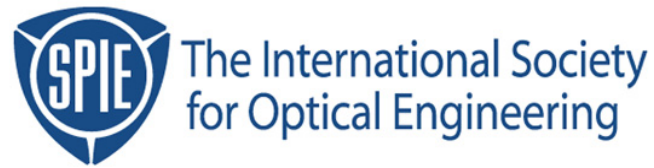


Copyright 2004 by the Society of Photo-Optical Instrumentation Engineers.



This paper was published in the proceedings of
Advances in Resist Technology and Processing XXI, SPIE Vol. 5376, pp. 322-332.
It is made available as an electronic reprint with permission of SPIE.

One print or electronic copy may be made for personal use only. Systematic or multiple reproduction, distribution to multiple locations via electronic or other means, duplication of any material in this paper for a fee or for commercial purposes, or modification of the content of the paper are prohibited.

The lithographic impact of resist model parameters

Mark D. Smith^{*}, Jeffrey D. Byers, Chris A. Mack
KLA-Tencor Corp.

ABSTRACT

The resist models in PROLITH are designed to be a mechanistic description of the resist chemistry and physics. This is especially true for the expose and post-exposure bake processes, where the resist chemistry can be mapped almost directly to the input parameters in the PROLITH models. In this study, we review the models in PROLITH and show how different chemistry parameters, such as the quantum yield and the reaction kinetics during PEB, can be translated into resist model parameters. With this “chemist to simulator” translator, we show how the models can be used to better understand how resist formulation impacts resist response. Specifically, we will show how quencher loading, and acid and quencher diffusivities impact depth of focus for isolated and dense features.

Keywords: Photoresist modeling, lithography simulation, PROLITH

1. INTRODUCTION

There are many different photoresist models that have been proposed, and these models range in complexity from very detailed, molecular-level descriptions of the resist to very fast, semi-empirical representations. It is useful to examine a few examples of each of the different types of photoresist models commonly used by lithographers today. Molecular-scale models of the photoresist include dynamic Monte-Carlo [1], molecular dynamics [2,3], and ab initio quantum calculations [4-6]. These models are useful for developing a deeper understanding of resist chemistry and physics from a molecular standpoint, and these models are typically used to determine how molecular structures impact bulk properties. For example, the ab initio quantum calculations in [6] were used to calculate the absorbance of various candidate polymer resins for 157nm resist formulations.

Continuum models of the photoresist are often used to determine the lithographic impact of bulk properties. Returning to the absorbance example, one might ask “What is the desired absorbance for a photoresist?” Conley et al [7] used the continuum resist models in PROLITH to determine the impact of a reduction of absorbance on the depth of focus for printing dense features at 193nm wavelengths. The general trends shown by the models were confirmed experimentally, and a maximum absorbance was proposed as a guideline for future photoresist formulations.

Using a model to optimize the resist absorbance is fairly straightforward because the relationship between the absorbance of the components of the resist and the inputs to the model is well-understood. The purpose of the current investigation is show how continuum models can be used to better understand other resist processing steps, such as PEB, and how these models might be used to engineer resist formulations for specific applications, such as printing isolated lines or trenches. This investigation has two basic parts. In Section 2, the models for expose, PEB, and develop will be reviewed and the connections between the resist chemistry and the model parameters will be highlighted. In Section 3, we will highlight the connection between the model parameters and their lithographic impact. This follows the same spirit as presented by Petersen [8] and Hansen [9]. Finally, in Section 4, the results in the first two sections will be used to show how a resist formulation might be optimized to print isolated lines, trenches, and contacts.

^{*} mark.d.smith@kla-tencor.com; phone 1-512-381-2318; 8834 North Capital of Texas Highway, Suite 301, Austin, TX 78759

2. GOVERNING EQUATIONS FOR EXPOSE, PEB, AND DEVELOP MODELS

The expose model in PROLITH consists of two parts. First, the intensity within the resist is calculated by solving the Maxwell equations within the film stack. The model parameters required for this step are the refractive index and absorbance for all of the materials on the wafer. These parameters can be measured using an ellipsometer, for example. The absorbance of the resist, α , is described by the Dill parameters A and B ,

$$\alpha = Am + B \quad (1)$$

where m is the relative concentration of the photoacid generator (PAG) molecule. The A parameter is called the bleachable absorbance, while the B parameter is called the unbleachable absorbance. The second part of the expose model in PROLITH is the photochemical decomposition of the PAG. This reaction is assumed to be first order in intensity (density of photons) and first order in the relative concentration of the PAG:

$$\frac{dm}{dt} = -CI(x, y, z)m \quad (2)$$

where C is the Dill parameter related to the photospeed. The translation of the A , B , and C parameters back into parameters relevant to the formulation of a photoresist is fairly straightforward:

$$A = 0$$

$$B = \frac{wt\% \cdot \rho \cdot \varepsilon}{MW} \cdot 2.303 \times 10^{-3} - \frac{\ln(\%T/100)}{d}$$

$$C = \frac{\varepsilon \cdot \phi}{N_A} \cdot \frac{\lambda}{h \cdot c} \cdot 2.303 \times 10^{-3}$$

where $\%T/d$ = polymer transparency
 MW = molecular weight of the PAG
 ε = PAG molar absorbance
 wt% = PAG concentration in weight percent
 ρ = the polymer density
 ϕ = quantum yield of the PAG

It is important to note that the absorbance is base e (not base 10) and that the bleachable absorbance, A , is typically zero for chemically amplified resists.

The input to the PEB model is the concentration of acid, H , at the end of the exposure step. This value is related to the unreacted photoacid generator by the equation

$$H = (1 - m)M_0 \quad (3)$$

where M_0 is the concentration of PAG at the beginning of the exposure step (the PAG loading). During PEB, the acid deblocks the polymer resin. This is described by a reaction-diffusion model, given by

$$\frac{\partial H}{\partial t} = \nabla \cdot (D_H \nabla H) - k_{loss} H - k_{quench} HQ \quad (4)$$

$$\frac{\partial Q}{\partial t} = \nabla \cdot (D_Q \nabla Q) - k_{quench} HQ \quad (5)$$

$$\frac{dW}{dt} = -k_{amp}HW \quad (6)$$

where D_H is the diffusivity of the acid, k_{loss} is the acid loss reaction rate constant, k_{quench} is the acid-base quench rate constant, Q is the concentration of base quencher, D_Q is the diffusivity of the base quencher, W is the concentration of blocked polymer sites, and k_{amp} is the deblocking reaction rate constant. We will also use the notation t_{PEB} to designate the duration of the PEB process.

In PROLITH (and most other photoresist simulators), the acid, quencher, and blocked polymer site concentrations are normalized to give the relative concentrations:

$$h = \frac{H}{M_0}$$

$$q = \frac{Q}{M_0}$$

$$w = \frac{W}{W_0}$$

where W_0 is the initial concentration of blocked polymer sites. This subtle change has an impact on the parameters in the PEB model described above:

$$\frac{\partial h}{\partial t} = \nabla \cdot (D_H \nabla h) - k_{loss} h - k_{quench} M_0 h q \quad (7)$$

$$\frac{\partial q}{\partial t} = \nabla \cdot (D_Q \nabla q) - k_{quench} M_0 h q \quad (8)$$

$$\frac{dw}{dt} = -k_{amp} M_0 h w \quad (9)$$

As shown in the above set of equations, all of the bimolecular reaction rates now contain an extra factor equal to the PAG loading, M_0 . In order to give a set of equations that resembles the original set of equations, we absorb the PAG loading into the k_{amp} and k_{quench} parameters to give the modified rate constants:

$$\frac{\partial h}{\partial t} = \nabla \cdot (D_H \nabla h) - k_{loss} h - K_{quench} h q \quad (10)$$

$$\frac{\partial q}{\partial t} = \nabla \cdot (D_Q \nabla q) - K_{quench} h q \quad (11)$$

$$\frac{dw}{dt} = -K_{amp} h w \quad (12)$$

While k_{amp} and k_{quench} are the values measured experimentally (ex, by FTIR measurements during the bake process), the parameters K_{amp} and K_{quench} are typically the values input into a lithography simulator. In PROLITH, K_{quench} is assumed to be very fast (instantaneous), so the only PROLITH parameter directly impacted by this change is the parameter K_{amp} . The translation of the PEB model parameters back into parameters relevant to the formulation of a photoresist is fairly straightforward:

$$M_0 = \frac{wt\% \cdot \rho}{MW}$$

$$Q_0 = \frac{(Qwt\%) \cdot \rho}{MW_Q}$$

$$K_{amp} = M_0 k_{amp}$$

where $Qwt\%$ is the quencher loading in weight percent, and MW_Q is the molecular weight of the quencher. The above results can be used to calculate the relative quencher loading (Q_0/M_0) for input into a PROLITH resist model. Finally, the diffusivities D_H and D_Q are typically very difficult to measure experimentally, but qualitatively, one might manipulate their values experimentally by changing the molecular weight and/or van der Waals volume of the PAG or quencher.

The final step in the PROLITH model is the develop process. The develop rate is assumed to be an empirical function of the protection level, w . There are many develop models that have been proposed. For simplicity, we will only consider the Mack develop equation [10]:

$$R(w) = R_{max} \frac{(a+1)(1-w)^n}{a+(1-w)^n} + R_{min}$$

$$a = \frac{(n+1)}{(n-1)} (1 - m_{th})^n$$

where the parameters R_{max} , R_{min} , n , and m_{th} are fit to match experimental develop rate data.

3. LITHOGRAPHIC IMPACT OF RESIST MODEL PARAMETERS

The models in the previous section involve many parameters, so it is useful to attempt to categorize the parameters according to the impact the parameters have on the lithographic response. This is similar to the approaches taken by John Petersen [8] and by Steve Hansen [9]. The categories here are all related to how the resist samples the intensity projected from the imaging tool. First, we consider the intensity at the feature edge, which is related to the photospeed-type parameters of the resist model. Second, we consider how the gradients in the intensity are converted into concentration and develop rate gradients. These parameters are contrast-type model parameters. Finally, we consider a type of response where the nominal feature edge is moved without impacting the photospeed or the contrast – these parameters impact the resist bias.

3.1 PHOTOSPEED PARAMETERS

The resist photospeed is measured by the dose-to-clear or the dose-to-size. While many resist model parameters impact the photospeed, only a few parameters affect photospeed without affecting other results. The main photospeed parameters are:

$$C, K_{amp}, Q, \text{ and } m_{th}$$

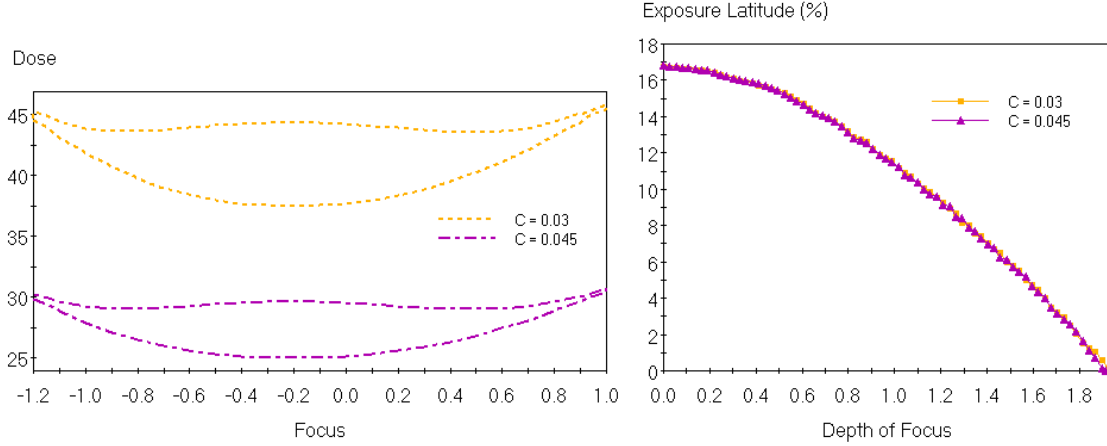


Figure 1: Process windows calculated for dense lines with all resist parameters and simulator settings the same except for the C parameter.

The only parameter that impacts photospeed without changing any other lithographic response is the Dill C parameter. As an example, two process windows are shown in Figure 1, where the only difference between the two models is the C parameters. As shown by the exposure latitude versus depth of focus plots, a change in the C parameter only impacts photospeed and does not change the shape of the process window.

3.2 CONTRAST PARAMETERS

Contrast parameters impact how a gradient in the intensity is converted into a gradient in acid concentration (at the end of expose), into a gradient in blocked polymer concentration (at the end of PEB), or into a gradient in the develop rate. We will consider a simple model to investigate the contrast parameters in our resist model. First, we start with an intensity profile that might arise from an alternating phase-shift mask:

$$I = I_o \left(1 + \cos \left[\frac{2\pi x}{L} \right] \right)$$

where L is the pitch of the mask. The concentration of photoacid at the end of expose will be given by

$$h = 1 - \exp \left\{ -cEI_o \left(1 + \cos \left[\frac{2\pi x}{L} \right] \right) \right\} \cong cEI_o \left(1 + \cos \left[\frac{2\pi x}{L} \right] \right)$$

From the above equation, we can conclude that the gradient in acid concentration is approximately proportional to the gradient in the intensity.

If no quencher is present, then the blocked polymer concentration after PEB can be determined from the above initial condition [11]. For the current derivation, we will also assume no loss reaction. This leads to

$$w = \exp \left\{ -K_{amp} cEI_o \left(t_{PEB} + \frac{1 - \exp \left(\left[\frac{2\pi}{L} \right]^2 D_H t_{PEB} \right)}{\left[\frac{2\pi}{L} \right]^2 D_H} \cos \left[\frac{2\pi x}{L} \right] \right) \right\}$$

Lastly, we assume that the relationship between develop rate and the blocked polymer fraction can be approximated by an exponential:

$$R = R_0 e^{\gamma w}$$

So that

$$\begin{aligned} \frac{\partial R}{\partial x} &= \gamma R \frac{\partial w}{\partial x} \\ &= R(\gamma w)(cEI_0) \left(K_{amp} \frac{1 - \exp\left(\left[\frac{2\pi}{L}\right]^2 D_H t_{PEB}\right)}{\left[\frac{2\pi}{L}\right]^2 D_H} \left[\frac{2\pi}{L}\right] \sin\left[\frac{2\pi x}{L}\right] \right) \end{aligned} \quad (13)$$

Finally, note that the image log-slope is equal to

$$\frac{1}{I} \frac{\partial I}{\partial x} = \left[\frac{2\pi}{L}\right] \sin\left(\frac{2\pi x}{L}\right)$$

When this is combined with a Taylor series expansion for the exponential in equation (13), we finally obtain:

$$\frac{\partial \ln R}{\partial x} = (cEI_0)(K_{amp} t_{PEB}) \left(1 - \left[\frac{2\pi}{L}\right]^2 \frac{D_H t_{PEB}}{2} \right) (\gamma w) \frac{\partial \ln I}{\partial x}$$

While this equation is fairly complicated, each term is related to a different part of the imaging process. The first term in parenthesis is related to the exposure dose, while the second term is related to the thermal dose required for the deblocking reaction. It is interesting to note that these terms usually have negligible impact on contrast – if one decreases C, for example, usually some other parameter, such as the dose or the PAG loading (hidden in K_{amp}) will need to be increased by the corresponding amount in order to achieve the correct target CD. The next two terms, however, have a large impact on the contrast – the develop rate contrast and the diffusivity during PEB. An increase in the develop rate contrast increases the overall contrast, while an increase in diffusivity decreases overall contrast.

3.3 RESIST BIAS

Petersen [8] defined the resist bias as the difference between the resist isofocal CD and the aerial image isofocal CD. The aerial image isofocal CD is shown in Figure 2 – this is the CD value that has a constant intensity value through focus. Shown in Figure 3 are focus exposure matrices calculated with a PROLITH resist model where the only difference in the models is the relative size of the acid and quencher diffusivities. As shown in figure, the resist bias is changes dramatically with the relative magnitudes of the acid and quencher diffusion coefficients. Previous studies have shown the impact of acid and quencher diffusion, such as Hattori et al who demonstrated better fits to CD data at best dose and focus, and by Lammers and van Steenwinkel [13] who experimentally demonstrated increased depth of focus for isolated lines and then used a simplified resist model with both acid and quencher diffusion to explain their results.

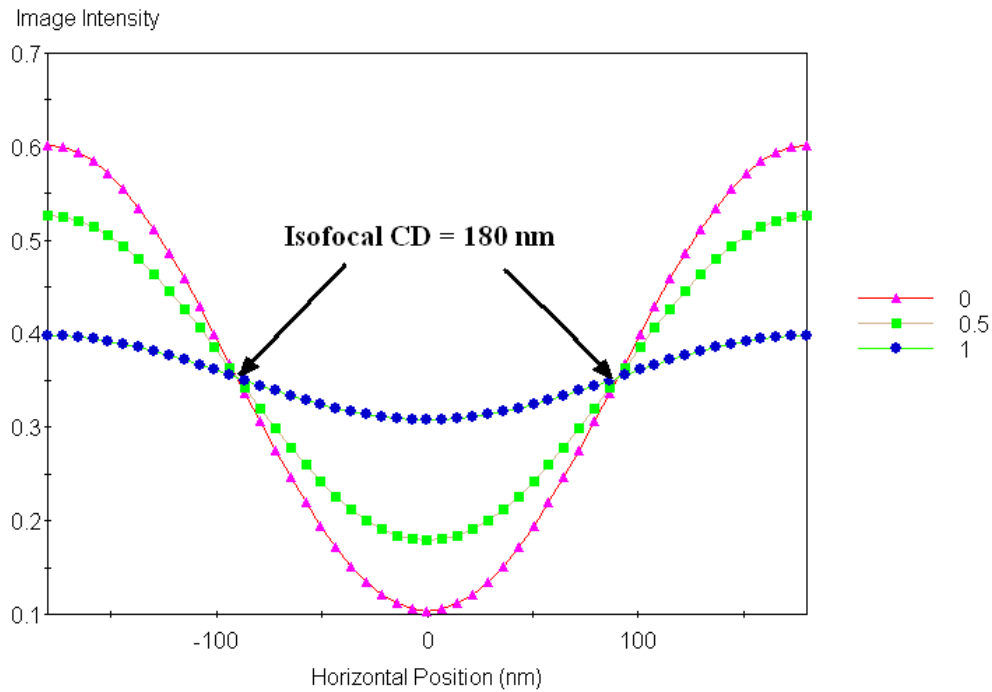


Figure 2: Calculated aerial images for a dense 180nm lines pattern on a 360nm pitch. Curves are shown for best focus and for 0.5 and 1.0 micron defocus. The isofocal CD for this set of aerial images is 180nm.

We explain the mechanism for the resist bias by a simple example. First, consider the intensity in resist for a simple lines-space pattern, as shown in Figure 4a. By using the exposure kinetics model outlined in the previous section, we can calculate the acid concentration at the end of the exposure process. This concentration will be the input to the PEB model, as shown in Figure 4b, where both the initial acid and the initial quencher concentrations are shown. In Figure 4c, the acid and quencher concentrations are shown after the initial acid-base neutralization reaction has occurred at the beginning of PEB. Figure 4d, the blocked polymer concentration is shown for the case where no acid or quencher diffusion is present. If we examine this final figure, it is clear that if acid diffusion were present, the acid would move inwards and act to reduce the width of the printed line, whereas if quencher diffusion were present, the quencher would

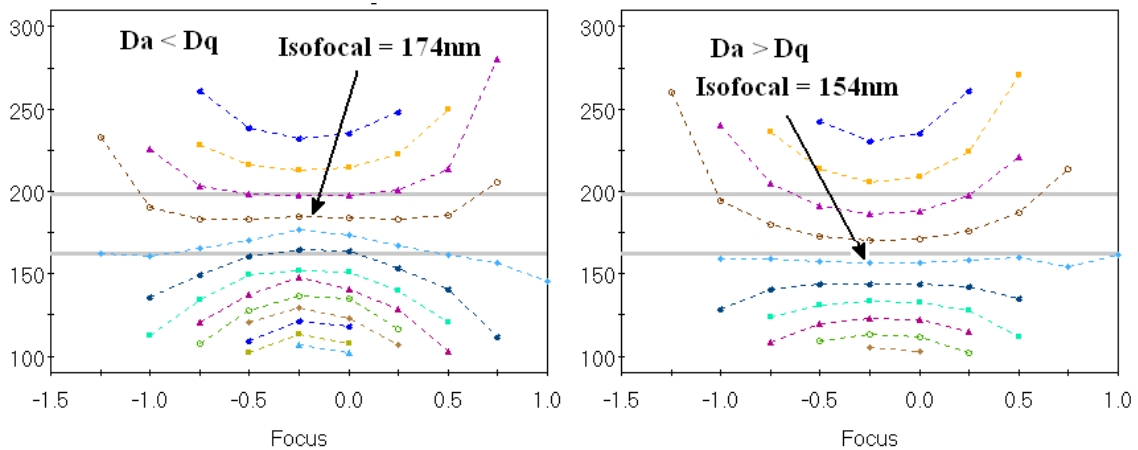


Figure 3: Calculated resist focus exposure matrices for the same pattern shown in Figure 2. On the left, the acid diffusivity is smaller than the quencher diffusivity and the resist bias is $174 - 180 = -6\text{nm}$. On the right, the acid diffusivity is larger, and the resist bias is $154 - 180 = -26\text{nm}$.

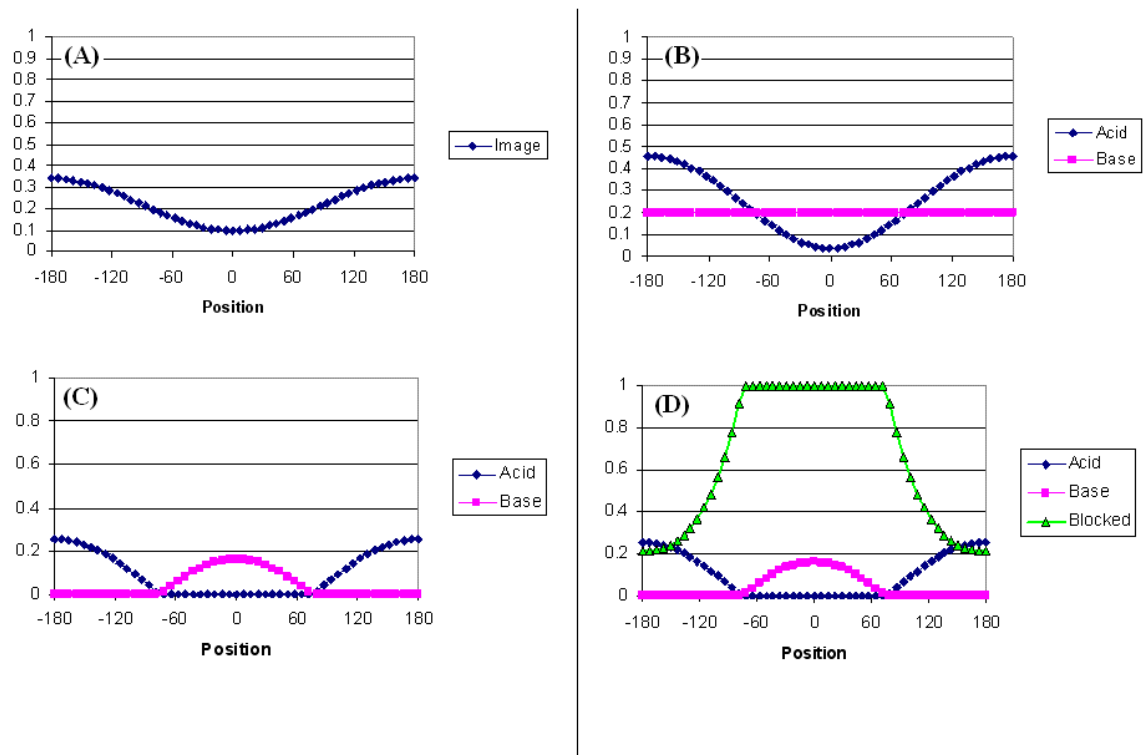


Figure 4: Step-by-step mechanism for the formation of the blocked polymer concentration. In (A), the intensity at the bottom of the resist is shown for a line-space pattern. In (B), the initial acid concentration generated by the exposure step is shown along with the initial quencher concentration. In (C), the initial acid-quencher neutralization reaction has occurred. In (D), the blocked polymer concentration is shown for the case where no acid or quencher diffusion is present.

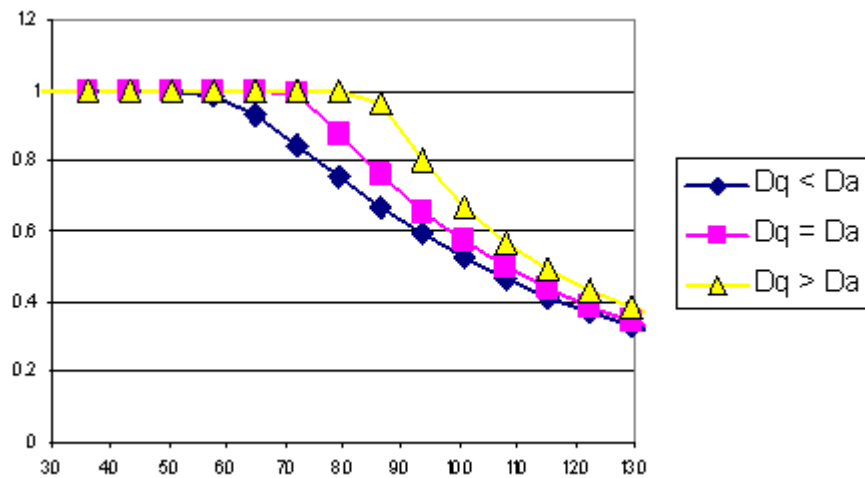


Figure 5: The blocked polymer concentration at the end of PEB for different relative values of the acid diffusivity and the quencher diffusivity. To show more detail near the feature edge, this figure only shows the right edge of the feature.

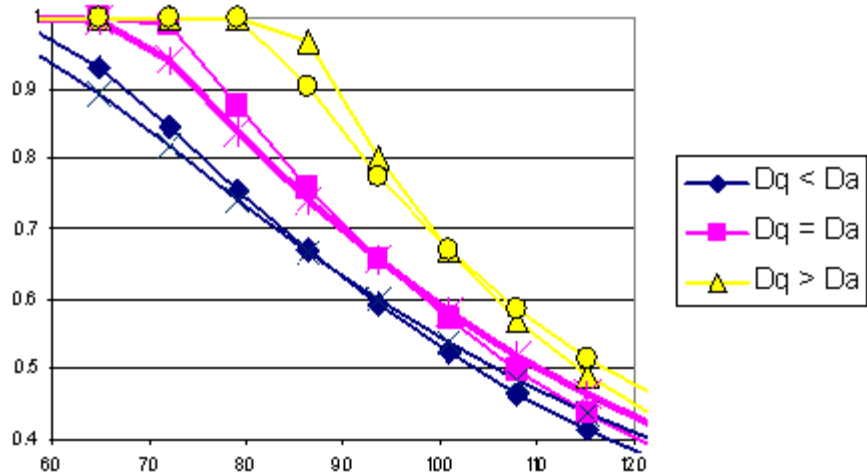


Figure 6: The blocked polymer concentration at the end of PEB for different relative values of the acid and quencher diffusivities. Results are shown for in-focus and for slightly out-of-focus images. The isofocal CD at the end of PEB for each condition can be seen where the two curves cross.

move inwards to neutralize the acid. This would cause less deblocking of the base resin, and the width of the printed line would increase. This is shown in Figure 5. Notice that the general shape of the three curves is the same – the difference is largely a “bias” which shifts the curve outwards as the relative quencher diffusivity is increased.

The impact of acid and base diffusion on the position of the isofocal is shown in Figure 6, where the same conditions are used as in Figure 5, except results are shown for in-focus and for out-of-focus images. The isofocal CD at the end of PEB is the position where the in-focus and out-of-focus curves cross. As shown in the figure, the isofocal CD increases as the relative amount of quencher diffusion is increased. The resist bias can also be clearly seen: the curves have the same general shape except that they are biased outwards as the amount of quencher diffusion increases. In addition to changing the bias, increased acid diffusion appears to also have an impact of the slope of the concentration curves in Figure 6. This is consistent with our categorization of the acid diffusivity as impacting both resist bias and resist contrast.

Finally, it is interesting to examine the impact of quencher loading on the resist bias. Obviously, if no quencher is present, the relative magnitude of the quencher diffusivity is irrelevant, but we should see the trends described in the previous paragraphs as the quencher loading is increased. So, we would expect the isofocal CD to also change dramatically with base loading. This is shown in Figure 7 for various quencher loadings and quencher diffusivities with all other resist parameters held fixed.

4. EXAMPLES OF MANIPULATING THE RESIST BIAS

A clear understanding of the mechanism of resist bias can be used to optimize a resist formulation to maximize depth-of-focus for different types of features. For example, for dense features, the aerial image isofocal will be approximately equal to half the pitch, so if one wants to print a 1:1 line-space pattern, the target CD will be very close to the aerial image isofocal and no resist bias is desired. For semi-isolated and isolated lines, the isofocal CD will be much larger than the target CD, so a large, negative resist bias will increase the DOF. This can be achieved by increasing acid diffusion. This approach has been demonstrated by Van Steenwinckel and Lammers [13], where the DOF of isolated lines was dramatically improved by using long PEB times. According to the mechanism outlined in the previous section, we expect that the acid diffusivity in this photoresist is large compared with the quencher diffusivity, and by baking for long PEB times the acid can diffuse inwards towards the center of the isolated lines. This should decrease the isofocal CD and improve DOF.

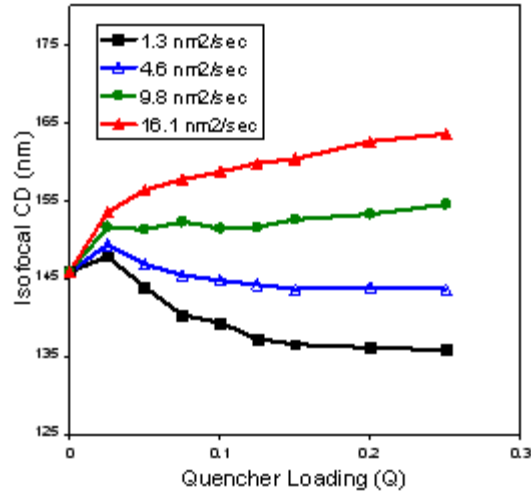


Figure 7: The impact of quencher loading on the isofocal CD for several different values of the quencher diffusion coefficient. These simulations were performed for XXXnm dense lines.

For contact holes, the resist bias has the opposite dependence on acid and quencher diffusivity because the tone of the feature has changed. For dark field features, a large, negative resist bias can be achieved by increasing the quencher diffusivity relative to the acid diffusivity.

5. SUMMARY AND CONCLUSIONS

In this study, we have reviewed the photoresist models in PROLITH, and shown how the different input parameters are related to the expose chemistry and the chemistry of the PEB process. Perhaps the most interesting relationship between resist formulation and lithographic performance is the resist bias, which provides an opportunity to improve the DOF for certain types of features. However, it is important to note that the different types of parameters (photospeed, contrast, and resist bias) are often coupled, so changing the resist bias will likely change contrast-related responses, such as the exposure latitude. Such complicated interactions are to be expected with advanced resist materials – a simple, straightforward resist model without these interactions would not resemble reality.

6. REFERENCES

1. G.M. Schmid, S.D. Burns, M.D. Stewart, C. Willson, "Mesoscale simulation of the lithographic process", *Proc. SPIE*, Vol. 4690 (2002).
2. M. Toriumi, T. Ohfuji, M. Endo, H. Morimoto, "Analysis of molecular diffusion in resist polymer films simulated by molecular dynamics", *Proc. SPIE*, Vol 3678 (1999) pp 368-379.
3. M. Toriumi, I. Okabe, T. Ohfuji, M. Endo, H. Morimoto, "Temperature dependence of acid molecular diffusion in resist polymer films simulated by molecular dynamics", *Proc. SPIE*, Vol 3999 (2000) pp. 1056-1061.
4. N.N. Matsuzawa, H. Oizumi, S. Mori, S. Irie, E. Yano, S. Okazaki, A. Ishitani, "Theoretical estimation of absorption coefficients of various polymers at 13nm", *J. Photopolym. Sci. Tech.*, Vol. 12 (1999) pp 571-576.
5. N.N. Matsuzawa, H. Oizumi, S. Mori, S. Irie, S. Shirayone, E. Yano, S. Okazaki, A. Ishitani, D.A. Dixon, "Theoretical calculation of photoabsorption of various polymers in the extreme ultraviolet region", *Jpn. J. Appl. Phys.*, Vol. 38 (1999), pp 7109-7113.
6. N.N. Matsuzawa, S. Mori, E. Yano, S. Okazaki, A. Ishitani, D.A. Dixon, "Theoretical calculations of photoabsorption of molecules in the vacuum ultraviolet region", *Proc. SPIE*, Vol. 3999 (2000), pp 375-384.
7. W. Conley, P. Zimmerman, D. Miller, G.S. Lee, "Imaging and Photochemistry Studies of Fluoropolymers for 193nm Lithography", *Proc. SPIE*, Vol 5039 (2003).
8. J.S. Petersen, Short Course: *Extending Semiconductor Lithography Resolution using Image Process Integration*
9. S.G. Hansen, "Resist vector: connecting the aerial image to reality", *Proc. SPIE*, Vol. 4690 (2002) pp. 366-380
10. C.A. Mack, *Inside PROLITH: A Comprehensive Guide to Optical Lithography Simulation*, FINLE Technologies, (Austin, TX: 1997)
11. M.D. Smith, C.A. Mack, "Examination of a simplified reaction-diffusion model for post-exposure bake of chemically amplified resists", *Proc. SPIE*, Vol. 4345 (2001) pp. 1022-1036.
12. K. Hattori, J. Abe, H. Fukuda, "The accuracy of simulation based on the acid-quencher mutual diffusion model in KrF process", *Proc. SPIE*, Vol. 4691 (2002) pp. 1243-1253.
13. D. Van Steenwinckel, J.H. Lammers, "Enhanced processing: sub-50nm features with 0.8 microns DOF using a binary reticle", *Proc. SPIE*, Vol 5039 (2003) pp. 225-239.